Magnetic field-assisted fission of a ferrofluid droplet for large-scale droplet generation

Haibo Zhao[1,2], Qiyu Deng[2], Tao Huang[2], Pingan Zhu[5], Wei Li[1], Xing Han[1], Xiang Li[2], Liqiu Wang[*1], Peng Yu[*2,3,4]

1) Department of Mechanical Engineering, The University of Hong Kong, Hong Kong, China

2) Department of Mechanics and Aerospace Engineering, Southern University of Science and Technology, Shenzhen, 518055, China

3) Guangdong Provincial Key Laboratory of Turbulence Research and Applications, Southern University of Science and Technology, Shenzhen,518055, China

4) Center for Complex Flows and Soft Matter Research, Southern University of Science and Technology, Shenzhen, 518055, China

5) Department of Mechanical Engineering, City University of Hong Kong, Hong Kong, China

*corresponding author (lqwang@hku.hk; yup6@sustech.edu.cn)

S1 Validation of the magnetic field of the permanent magnet

For a cylinder permanent magnet, the magnetic induction strength B, and the distance from one point along the central axis to the magnet surface h satisfy:

$$B(h)=\frac{B_r}{2}\left(\frac{t+h}{\sqrt{\left(\frac{d}{2}\right)^2+(t+h)^2}}-\frac{h}{\sqrt{\left(\frac{d}{2}\right)^2+h^2}}\right), \tag{S1}$$

where B_r is the residual magnetic field of the magnet, t is the thickness, and d is the diameter. The maximum magnetic induction strength B_{max} measured at the center of the magnet surface is 220 mT. B_r can be deduced from the maximum magnetic induction strength B_{max} by $B(0) = B_{max}$. Fig. S1(a) plots the measured and the analytical B at different h. The magnetic magnitude rapidly decreases with the distance until it reaches the near-zero value at the far point. It is observed that the measured values agree well with the analytical data. The gradient of the external magnetic magnitude along the z axis is also calculated and shown in Fig. S1(b). The magnitude reduction rate decreases with h. The relation between B and its gradient is demonstrated in Fig. S1(c), which shows that B increases with ∇B.

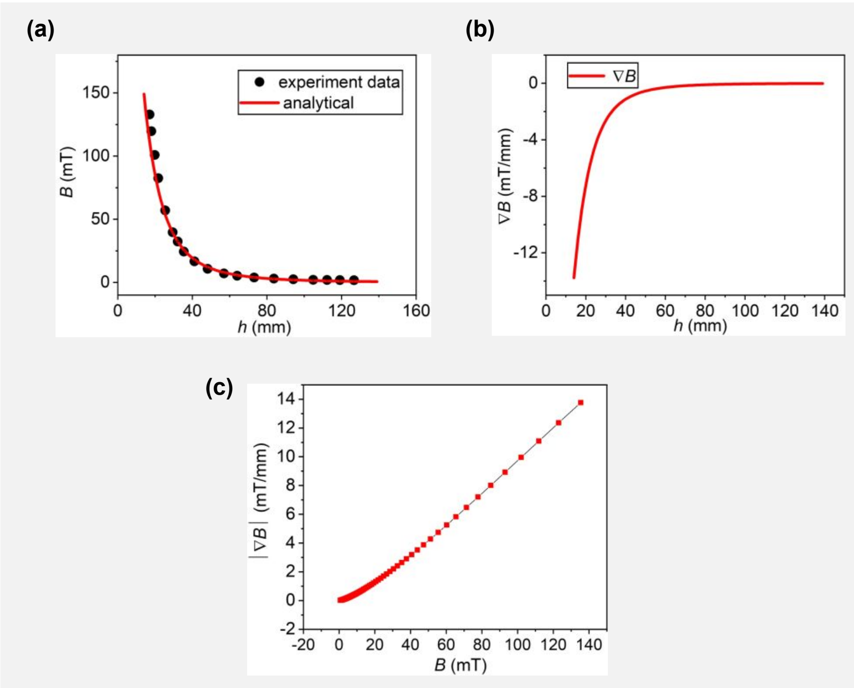

Fig. S1 (a) The spatial variation of the magnetic induction strength along the z direction. Black dots represent the experimental data and the solid line is the analytical result. (b) The gradient of B along the z direction. (c) The relationship between B and ∇B.

S2 Ferrofluid droplet fission under static state

Rosensweig stability is commonly observed when applying a perpendicular uniform magnetic field to a pool of ferrofluid [1]. It produces an ordered pattern of surface peaks with a critical wavelength $\lambda_c = 2\pi\sqrt{\sigma/\rho g}$, where σ is the surface tension coefficient, ρ is the ferrofluid density, and g is the gravity acceleration. In addition, the magnetization should exceed the critical threshold M_c, $M_c^2 = \frac{2}{\mu_0}\left(1+\frac{\mu_0}{\mu}\right)\sqrt{\rho g \sigma}$, where μ_0 (μ) is the magnetic permeability at vacuum (ferrofluid). When applying a permanent magnet beneath the ferrofluid droplet, due to the vertical field gradient, the ferrofluid droplet experiences the additional magnetic force $\frac{d}{dz}(\mu_0 HM)$. The droplet fission process occurs if the droplet characteristic length is larger than the revised critical wavelength $\lambda_c^* = 2\pi\sqrt{\sigma\Big/\left(\rho g + \frac{d}{dz}(\mu_0 HM)\right)}$. Fig. S2(a) demonstrates the droplet fission process when the magnet approaches the solid surface[2]. This critical length no longer means the periodicity of the pattern but rather indicates the criterion for droplet fission. When a droplet, with initial volume V_0, is split into N_s daughter droplets, the equivalent radius $d_e = \left(\frac{6V_0}{N_s\pi}\right)^{1/3}$ should satisfy the condition $d_e \approx \lambda_c^*$. Thus, the daughter droplet number and the critical length satisfy the relationship $N_s \sim V_0 {\lambda_c^*}^{-3}$. This relationship indicates that the number of daughter droplets decreases with the critical wavelength. Fig. S2(b) plots the $H \sim N_s$ relationship both for the experimental data (red dots) and the analytical result (black solid line). It could be observed that the relationship $N_s \sim V_0 {\lambda_c^*}^{-3}$ is in good agreement with the experimental results.

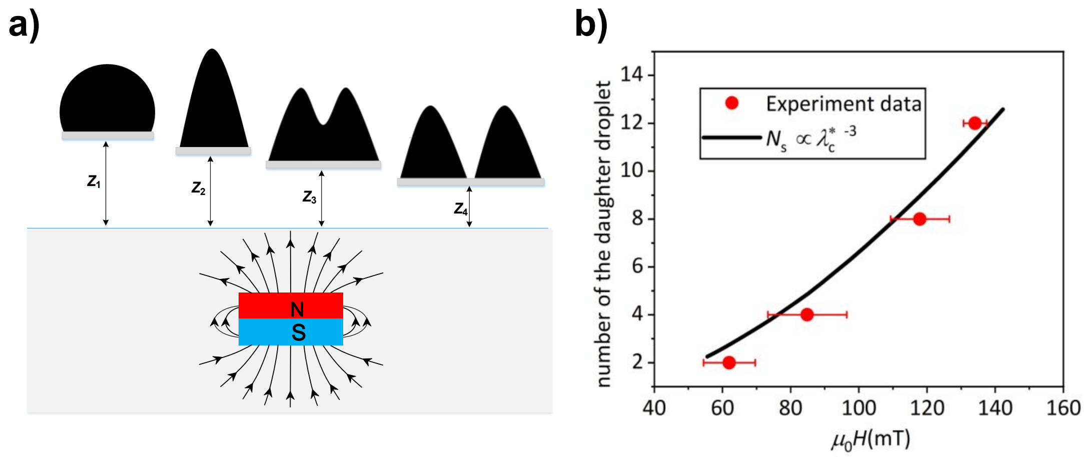

Fig. S2 (a) The static ferrofluid droplet fission process when the magnet approaches the solid surface. z_1, z_2, z_3, and z_4 are the distance between the magnet and the static droplet, with $z_1 > z_2 > z_3 > z_4$. (b) The relation between the number of the daughter droplet and H on the solid surface for the experimental data (red dots) and the analytic result (black solid line).

S3 The calculation of the magnetic force exerted on the ferrofluid droplet

For a linear ferrofluid whose density and magnetization have a linear relationship, the magnetic body force is the kelvin force and calculated as[3],

$$F_{\mathrm{M}} = -\mu_0 M \nabla H_{\mathrm{i}}, \tag{S2}$$

where M is the magnetization and H_{i} is the magnetic field strength inside the ferrofluid droplet. Herein, H_{i} is an induced field because the presence of the ferrofluid droplet modifies the applied exernal magnetic field H. The relationship between H_{i} and H can be expressed as,

$$\mathrm{H_i} = \mathrm{H} - NM, \tag{S3}$$

where N is the demagnetization factor and is solely dependent on the droplet shape. When the shape is spherical, N equals 1/3.

For simplicity, a linear relation for the magnetization is adopted,

$$\mathrm{M} = \chi \mathrm{H_i}, \tag{S4}$$

where χ is the magnetic susceptibility. Substituting Eq. (S4) into Eq. (S3) yields:

$$\mathrm{H_i} = \frac{\mathrm{H}}{1 + N\chi} \tag{S5}$$

Substituting Eq. (S5) into Eq. (S2) and assuming that H is distributed along the z direction, we obtain the expression of the magnetic body force utilized in the present work,

$$F_{\mathrm{M}} = -\mu_0 \frac{\partial \mathrm{H}}{\partial z} \frac{M}{1 + N\chi} \tag{S6}$$

Herein, N and χ are assumed to be irrespective of the position.

S4 Movies

Movie S1

A ferrofluid droplet is stretched along the *z* direction and deformed from sphere to elliptical shape. The magnetic induction strength near the solid surface is 10.87 mT and the impact velocity is 0.66 m s^{-1}.

Movie S2

A ferrofluid droplet impacts on a superhydrophobic surface without the magnetic field. The impact velocity is 0.99 m s^{-1}. The maximum spreading diameter is 5.9 mm.

Movie S3

A ferrofluid droplet impacts on a superhydrophobic surface with the presence of a magnetic field. The impact velocity is 1.0 m s^{-1} and the magnetic induction strength near the solid surface is 16.7 mT. The maximum spreading diameter is 5.0 mm.

Movie S4

A ferrofluid droplet impacts on a superhydrophobic surface with the magnetic induction strength near the solid surface 3.96 mT and the impact velocity of 0.85 m s^{-1}. The droplet undergoes the spreading-retraction-rebounding and breakup process.

Movie S5

A ferrofluid droplet impacts on a superhydrophobic surface with the magnetic induction strength near the solid surface 16.7 mT and the impact velocity of 1.31 m s^{-1}. The droplet experiences the rim instability in the receding process and no daughter droplet appears eventually.

Movie S6

A ferrofluid droplet impacts on a superhydrophobic surface with the magnetic induction strength near the solid surface 40.5 mT and the impact velocity of 1.25 m s^{-1}. The droplet experiences the rim instability in the spreading stage and the fission process completes before retraction. Eventually, the daughter droplets with evenly-distributed size form.

Movie S7

A ferrofluid droplet impacts on a superhydrophobic surface with the magnetic induction strength near the solid surface 32.57 mT and the impact velocity of 2.65 m s^{-1}. The droplet experiences the rim instability in the later spreading stage and forms the fingers. Some fingers complete the fission process and become tiny daughter droplets. The remained fingers retract centripetally and aggregate into one larger droplet. Eventually, the daughter droplets with unevenly-distributed size form.

Movie S8

The top view of a ferrofluid droplet impacting on a superhydrophobic surface. Eventually, the daughter droplets with uniform size form. There are also some very small daughter droplets and these droplets result from the filaments connecting the daughter droplets with main part of the mother droplet.

Movie S9

The top view of a ferrofluid droplet impacting on a superhydrophobic surface. Eventually, the daughter droplets with non-uniform size form.

Reference

(1) COWLEY, M. D.; ROSENSWEIG, R. E. The Interfacial Stability of a Ferromagnetic Fluid. *J. Fluid Mech.* **1967**, *30*, 671–688.

(2) Timonen, J. V. I.; Latikka, M.; Leibler, L.; Ras, R. H. A.; Ikkala, O. Switchable Static and Dynamic Self-Assembly of Magnetic Droplets on Superhydrophobic Surfaces. *Science* **2013**, *341* (6143), 253–257.

(3) Rosensweig, R. E. *Ferrohydrodynamics*; Cambridge University Press: Cambridge, 1985.